Indian Ocean SST and Indian Summer Rainfall: Predictive Relationships and Their Decadal Variability

CHRISTINA OELFKE CLARK

Program in Atmospheric and Oceanic Sciences, University of Colorado, Boulder, Colorado

JULIA E. COLE*

Department of Geological Sciences/INSTAAR/PAOS, University of Colorado, Boulder, Colorado

PETER J. WEBSTER

Program in Atmospheric and Oceanic Sciences, University of Colorado, Boulder, Colorado

(Manuscript received 2 October 1998, in final form 23 August 1999)

ABSTRACT

The authors examine relationships between Indian Ocean sea surface temperature (SST) variability and the variability of the Indian monsoon, including analysis of potential long-lead predictions of Indian rainfall by regional SST and the influence of ENSO and decadal variability on the stability of the relationships. Using monthly gridded (4° × 4°) SST data from the Global Sea-Ice and Sea Surface Temperature (GISST) dataset that spans 1945–94, the correlation fields between the All-India Rainfall Index (AIRI) and SST fields over the tropical Indian Ocean are calculated. In the boreal fall and winter preceding the summer Indian monsoon, SST throughout the tropical Indian Ocean correlates positively with subsequent monsoon rainfall. Negative correlation occurs between SST and the AIRI in the subsequent autumn in the northern Indian Ocean only. A strong correlation (0.53) is found between the summer AIRI and the preceding December–February Arabian Sea SST. The correlation between the AIRI and the SST to the northwest of Australia for the same period is 0.58. The highest correlation (0.87) for the years following 1977 is found between the AIRI and the central Indian Ocean SST in the preceding September–November, but this relationship is much weaker in earlier years. Based upon these correlations, the authors define Arabian Sea (AS1), northwest Australia (NWA1), and central Indian Ocean (CIO1) SST indexes. The relationships of these indexes to the AIRI and ENSO are examined. The authors find that the high correlation of the AS1 and NWA1 SST indexes with the Indian summer rainfall is largely unaffected by the removal of the ENSO signal, whereas the correlation of the CIO1 index with the AIRI is reduced. The authors examine the interdecadal variability of the relationships between SST and the AIRI and show that the Indian Ocean has undergone significant secular variation associated with a climate shift in 1976. The possible mechanisms underlying the correlation patterns and the implications of the relationship to the biennial nature of the monsoon and predictability are discussed.

1. Introduction

The Asian monsoon circulation influences most of the tropics and subtropics of the Eastern Hemisphere and more than 60% of the earth's population (Webster et al. 1998). Monsoon variations, particularly if they are unanticipated, impart significant economic and social consequences. Monsoon failure often brings famine to affected regions, and strong monsoon years can result in devastating floods. An accurate long-lead prediction of monsoon rainfall can improve planning to mitigate the adverse impacts of monsoon variability and to take advantage of beneficial conditions (Webster et al. 1998). A better understanding of the monsoon cycle is clearly of scientific and social value. Monsoon prediction studies have utilized indicators of atmospheric circulation, land surface conditions, and Indian and Pacific Oceans SSTs (summarized in Webster et al. 1998). The predictive relationship between Indian Ocean SST and monsoon rainfall remains especially poorly characterized, particularly at lead times greater than 1–2 months before the boreal summer monsoon season. This study assesses the relationship between SST variations in the tropical

* Current affiliation: Department of Geosciences, The University of Arizona, Tucson, Arizona.

Corresponding author address: Christina Clark, Program in Atmospheric and Oceanic Sciences, Campus Box 311, University of Colorado, Boulder, CO 80309-0311.
E-mail: oelfke@bogart.colorado.edu

Indian Ocean and Indian monsoon rainfall, including the temporal stability of these linkages over the past 50 yr with the goal of improving multivariate monsoon prediction efforts.

a. Monsoon variability

The Asian monsoon is characterized by a seasonal reversal of surface winds and a distinct seasonality of precipitation. During the boreal summer, winds flow from the Southern Hemisphere, accumulating moisture and depositing copious amounts of precipitation over the south Asian continent. In the winter, dry winds flow from the cold land areas of Asia southwest toward the warm southern ocean. These winds converge over the warm Southern Hemisphere ocean, Indonesia, and the north Australian continent to produce the precipitation of the Australian monsoon. The fundamental driving mechanisms of the monsoon cycle are the cross-equatorial pressure gradients resulting from differential heating of land and ocean, modified by the rotation of the earth and the exchange of moisture between the ocean, atmosphere, and land (e.g., Webster 1987). The Himalayas and the Tibetan Plateau provide additional strong thermal forcing that produces a distinct asymmetry to the summer monsoons of the Northern and Southern Hemispheres (Yanai and Li 1994; Webster et al. 1998). In addition to the strong seasonality of wind and rainfall patterns, the monsoon regions also experience a high degree of variability on intraseasonal, interannual, and interdecadal timescales. The timing of the onset date of the summer rainfall in a particular location can vary considerably from one monsoon season to the next, and the rainfall over large regions can experience ''breaks'' in activity within a season, during which there is little or no precipitation (Webster et al. 1998 and references therein). Such intraseasonal oscillations occur with timescales of weeks.

On interannual timescales, the Asian monsoon exhibits a fairly distinct bienniality. A spectral analysis of Indian rainfall shows peaks in the 2–3-yr period range (Mooley and Parthasarathy 1984). Years of heavy rainfall tend to be followed by years of diminished rainfall. This biennial component is known as the tropospheric biennial oscillation (TBC) and appears in a wide range of atmospheric variables including rainfall, surface pressure, wind, and SST (Meehl 1987). The origin of the TBO is a subject of debate. Meehl (1997) described an air–sea negative feedback mechanism in which warm spring SSTs in the Indian Ocean enhance atmospheric convection. The ensuing stronger monsoon leads to greater than average wind strength, increased Ekman transports and vertical mixing, and higher heat loss by evaporation throughout the summer monsoon season, which causes subsequent cooling of the ocean surface. The low ocean temperatures persist for one year until the next pluvial season. The lowered SSTs are associated with less convection than the previous spring, producing weakened winds, reduced heat loss by evaporation, and less mixing, which leads to higher SSTs than the year before. The cycle is thus repeated. The strength of the TBO is modulated by interdecadal variability. For example, Torrence and Webster (1999) find the biennial oscillation to be weaker in some decades than others.

Another potential explanation for biennial monsoon variability involves land surface processes, especially Eurasian snow cover. Extensive snow cover typically precedes a weak monsoon and light snow cover precedes a strong monsoon (Barnett et al. 1989; Yang 1996; Vernekar et al. 1995). Large and persistent winter snow cover over Eurasia following a strong monsoon can delay and weaken the spring and summer heating of landmass that is necessary for the establishment of large-scale monsoon flow (Shukla 1987; Barnett et al. 1989; Yasunari et al. 1991). In this manner, snow cover may act as a negative feedback upon the Asian monsoon, imparting biennial variability. Clearly a better understanding of the ocean–atmosphere and land–atmosphere feedbacks that may give rise to the TBO can improve predictions of monsoon strength.

On interannual and longer timescales, the variability of the Asian monsoon is linked with the El Niño–Southern Oscillation (ENSO). The occurrence of El Niño is generally associated with a weak monsoon, and La Niña is associated with a strong monsoon (e.g., Webster and Yang 1992). During normal periods, the warm pool (SST $>$ 27°C) extends from the eastern Indian Ocean to the western Pacific Ocean and is associated with a broad precipitation maximum. During an El Niño event, the locus of maximum SST in the Pacific Ocean shifts eastward, typically bringing more precipitation over the central and eastern Pacific Ocean. During these periods the eastern Indian Ocean, Indonesia, and south Asia are in the subsiding part of the Walker circulation that has shifted eastward from its climatological position (Webster et al. 1998). Between 1871 and 1994, there were 22 deficient Indian rainfall events (rainfall $>$ 1 standard deviation below mean), 11 of which occurred during an El Niño episode and 2 of which occurred during La Niña. In this same period, there were 18 events of heavy rainfall, 7 of which occurred during La Niña, but none occurred during El Niño (Webster et al. 1998). Clearly, there is a connection between the Asian monsoon and ENSO, but it is not possible to predict the strength of the monsoon solely from the phase of ENSO, as these monsoon–ENSO correlations have variable lag-lead times (Webster and Yang 1992). In addition, the connection between the Asian monsoon and ENSO appears to be statistically nonstationary (e.g., Troup 1965). The correlation between Indian rainfall and Pacific Oceans SST varies from 0.4 to 0.8 for different decades from 1900 through to the present (Torrence and Webster 1999). Wavelet analysis shows that from 1920 to 1960, the Southern Oscillation index (SOI) was comparatively quiescent, yet the variability of Indian rainfall was not significantly reduced. With regard to monsoon–ENSO

relationships, Torrence and Webster (1999) substantiate the findings of Troup (1965) and note the demise of ENSO-based predictive relationships in the 1920–60 period. During the last decade, the ENSO–monsoon relationship has also weakened. During the 1993/94 and 1997/98 El Niño events, the Indian rainfall remained essentially normal (Webster et al. 1998; Torrence and Webster 1999).

On interdecadal timescales, the tropical climate system also experiences secular changes. One such climate shift occurred in 1976 and is characterized by significant changes in the structure and evolution of ENSO (Trenberth 1990; Graham 1994; Wang 1995). After 1976, there occurred more El Niño and fewer La Niña events than in previous years (Trenberth 1990; Trenberth and Hoar 1996). Significant SST increases were found in the tropics of the central and eastern Pacific and Indian Oceans and were linked to enhanced convective activity (Nitta and Yamada 1989). Empirical orthogonal function (EOF) analysis performed on the tropical Pacific and Indian Oceans SST shows a rapid transition from a cold to warm state in the late 1970s (Wang 1995). A comparison between land and marine datasets in the Indian Ocean reveals a sudden warming of SST after 1976 and corroborates the evidence of a climatic change in the Indian Ocean after 1976 (Terray 1994). Our study demonstrates that this climate shift alters the correlation structure between Indian Ocean SST fields and subsequent Indian monsoon rainfall.

b. The role of the Indian Ocean

Gradients of SST within the oceans are important in determining the location of precipitation over the Tropics, including the monsoon regions (Lindzen and Nigam 1987). As a first approximation, it might be supposed that the distribution of SST in the Indian Ocean plays a role in determining monsoon rainfall variability. The influence of the tropical oceans on the Asian monsoon has been suggested by models and empirical evidence. Atmospheric general circulation models (GCMs) have been used to address how the regional climate associated with monsoon rainfall and circulation anomalies responds to imposed SST anomalies. The Monsoon Numerical Experimentation Group (MONEG) of the World Climate Research Programme (WCRP) attempted to replicate the contrasting monsoon seasons of 1987 and 1988 using variable ocean boundary conditions (Sperber and Palmer 1996). Seventeen atmospheric modeling groups ran 90-day integrations using the observed global SST fields for 1987 and 1988 as boundary forcing and the atmospheric fields as initial conditions (World Climate Research Programme 1992). The difference between estimates of monsoon rainfall by the different models was systematic, either universally high or low. This systematic difference suggests that the Indian Ocean region is difficult to model, perhaps because of the strong seasonal SST gradients and consequently spatially steep heating gradients. There is also a great difference in the manner in which each model simulates the mechanical and heating effects of the Tibetan Plateau. Given the importance of this mountain complex (e.g., Yanai and Li 1994), it is not surprising that simulations of precipitation close to the Himalayas were different among models. However, multiple runs by the European Centre for Medium-Range Weather Forecasts (ECMWF) models starting with different initial conditions also showed a dispersion in the mean seasonal precipitation (Sperber and Palmer 1996), indicating that local monsoon instabilities may be important (Webster et al. 1998).

Several additional studies demonstrate the significance of the Indian Ocean SST in influencing the monsoon. A GCM study in which the solar forcing of the land and ocean are incorporated separately shows that the annual cycle of SST in the Indian Ocean is crucially important in establishing the monsoon circulation and rainfall (Shukla and Fennessy 1994). Model simulations also confirm that the Arabian Sea SST influences subsequent monsoon rainfall on timescales less than a month. A cool Arabian Sea SST leads to reduced Indian rainfall and vice versa (Shukla 1975; Kershaw 1988; Yang and Lau 1998).

c. Monsoon prediction

Empirical forecasting of Indian monsoon rainfall has been performed using combinations of climatic parameters, including atmospheric pressure, wind, snow cover, SST, and the phase of ENSO (e.g., Parthasarathy et al 1988; Shukla and Mooley 1987; Hastenrath 1986; Hastenrath 1987; Wu 1985; Harzallah and Sadourny 1997; Sadhuram 1997). Regression models based on these and other empirical correlations have been able to predict 60%–80% of the total seasonal Indian rainfall by the May preceding the summer monsoon (Hastenrath 1994).

A goal of this research is to describe Indian Ocean–monsoon relationships that will contribute to the prediction of rainfall at lead times significantly longer than the May preceding the onset of the south Asian summer monsoon. Several studies document empirical links between Indian Ocean SST and monsoon variability. Negative correlations exist between the all-India rainfall index (AIRI) (defined by Parthasarathy et al. 1992) and the Indonesian SST 16 months earlier (Nicholls 1983). These negative correlations change sign in November and December and reach the 95% significance level ($r = 0.51$) in the February preceding the Indian monsoon. Several other empirical studies show a strong positive correlation of Arabian Sea SST averaged over March, April, and May with Indian summer rainfall (Shukla and Mooley 1987; Joseph and Pillai 1984; Rao and Goswami 1988; Allan et al. 1995). Harzallah and Sadourny (1997) investigate lag-lead relationships of global SST and the AIRI from 1950–90. They find that positive SST anomalies exist in the Indian Ocean, especially the

Arabian Sea, in the fall and winter preceding a strong monsoon. A strong correlation (0.75) exists between Indian rainfall and SST in the central Indian Ocean in the October and November preceding the monsoon for the years 1967–87 (Sadhuram 1997). Thus, Indian Ocean SST variability holds promise for improved predictions of monsoon rainfall.

Our study further explores the relationship between Indian Ocean SST and monsoon rainfall, including its connection to ENSO. We calculate the monthly correlation of summer rainfall over India with SST at all locations within the tropical Indian Ocean and evaluate the stability of these relationships over the period of 1945–95. Specific regions where winter SST correlates with the subsequent AIRI include the Arabian Sea, a region northwest of Australia, and the central Indian Ocean; these results confirm previous studies that used different SST datasets (Harzallah and Sadourny 1997; Sadhuram 1997). We expand upon these studies by examining the influence of ENSO on the SST–AIRI correlation and by exploring the interdecadal variability of these correlations. We define indexes of three-month average SST values extracted from three locations within the Indian Ocean where the correlations with the AIRI are the strongest. We show that the central Indian Ocean has undergone a shift in its relationship with the AIRI in 1976, after which time its correlation with the AIRI is much stronger; other regions show correlations that remain stable over the period of analysis. Although ENSO has a strong signature in the Indian Ocean, removal of the ENSO signal from the SST indexes does not strongly affect the correlations of the AIRI with SST from the Arabian Sea and the region northwest of Australia, but it does decrease the correlation of the AIRI with SST in the central Indian Ocean. This decrease is not surprising because the maximum correlation between the Indian Ocean SST and Niño-3 SST occurs in the central Indian Ocean.

2. The data

The basic SST dataset used in this study is the global sea-ice and sea surface Temperature (GISST, version 2.4) dataset compiled from ship records (Parker et al. 1995). These data contain a global record of monthly SST from 1880 to the present, although optimum coverage has been reached only since 1945. A grid ($4° \times 4°$) of monthly SST from 1945 to 1997 is used with the average annual cycle removed, and we restrict our analysis to the tropical Indian Ocean in the range 24°S–24°N and 40°E–120°E. We use the Niño-3 SST index to represent the strength of ENSO; Niño-3 is the area-average SST over the eastern equatorial Pacific (5°S–5°N, 90°–150°W; Bjerknes 1969). The annual AIRI, the rainfall over the Indian subcontinent totalled annually from June through September (JJAS; Parthasarathy et al. 1992), has been computed for the past century and has been used as an indicator of the strength of the Indian monsoon. The AIRI consists of an area-weighted average of 306 rain gauges distributed across India.

A linear least squares fit to the GISST dataset at each grid point within the tropical Indian Ocean was performed (Fig. 1). The Indian Ocean SST is dominated by a strong positive trend, with the strongest warming, greater than 0.02°C yr^{-1} in the equatorial Indian Ocean west of Indonesia (Fig. 1b). Averaging the GISST dataset over the tropical Indian Ocean region (defined above) produces the timeseries shown in Fig. 1a. A linear fit of this timeseries reveals an average warming trend from 1945 to 1997 of one degree per century. Removal of this trend reduces the total variance of the timeseries by 31%. In agreement with Terray (1994), it is found that most of the warming in the Indian Ocean has occurred after 1976, with a linear trend of 0.01°C yr^{-1} (Fig. 1a, dotted line), whereas during the period from 1945 to 1976, the warming was only 0.003°C yr^{-1}. Although the warming is weak throughout the Indian Ocean prior to 1976 (Fig. 1c), the trend is greater than 0.03°C yr^{-1} in the central Indian Ocean and in Indonesia after 1976 (Fig. 1d). We have removed the trend at each grid point to simplify the correlation analyses in this study. Removal of the trend is found to strengthen correlations of SST with Indian summer rainfall by 0.01 to 0.2.

Although the long-term SST trend is not central to the current study, it is important to recognize its potential significance to the character of the evolution of the monsoon regime. Most of the temperature increases have occurred in the last 20 yr corresponding to the epochal changes described by Trenberth (1990), Graham (1994), and Wang (1995). Given the uncertainties of the datasets and their limited length, it is difficult to know whether the increases in the Indian and Pacific SSTs are part of natural interdecadal oscillations or are caused by anthropogenic effects. The long-term variations could help explain the nonstationary aspect of the monsoon–ENSO connection.

3. Results

a. SST–Indian rainfall relationships, 1945–95

To determine the monthly SST–annual AIRI relationship preceding and following the monsoon, we correlate the SST timeseries for each month at each grid point in the Indian Ocean with the AIRI beginning with the June, 12 months (i.e., four seasons) prior to the AIRI. A similar analysis was performed by Harzallah and Sadourny (1997) using global MOHSST4 SST data (Bottomley et al. 1990). The correlation of 3-month average SST fields with the JJAS AIRI beginning one year prior to the AIRI are shown in Fig. 2. For 50 yr of data, the 95% and 99% significance levels are 0.28 and 0.36, respectively, using a Student's t-distribution. The SST throughout the entire Indian Ocean is positively correlated with the AIRI throughout the fall, winter, and early spring preceding

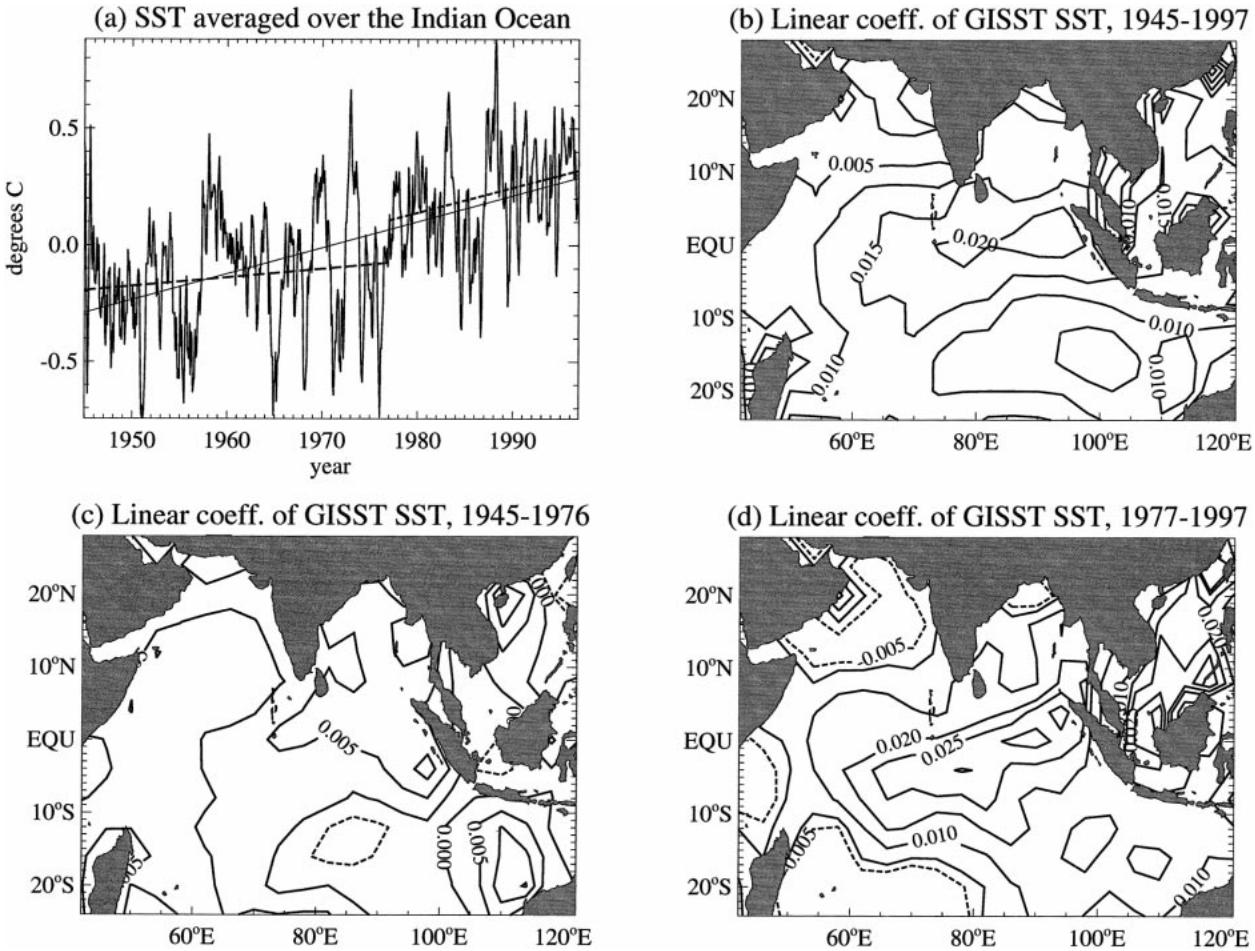

FIG. 1. Variability of Indian Ocean SST in the period of 1945–97. (a) Time series of SST averaged over the tropical Indian Ocean north of 24°S. The solid line is a linear least squares fit from 1945 to 1997, with a slope of 0.01°C yr^{-1}. The dashed line is a linear fit from 1945 to 1976, with a slope of 0.003°C yr^{-1}. The dotted line is a linear fit from 1977 to 1997, with a slope of 0.01°C yr^{-1}. (b) Linear coefficient of GISST SST (Parker et al. 1995) from 1945 to 1997. (c) Linear coefficient of GISST SST from 1945 to 1976. (d) Linear coefficient of GISST SST from 1977 to 1997.

the Indian summer monsoon, confirming earlier results (Harzallah and Sadourny 1997, their Fig. 3). This positive correlation weakens prior to and during the onset of the summer rainfall, and negative correlations emerge in the northern Indian Ocean in the subsequent fall. This result agrees with numerical modeling experiments (Shukla 1975; Yang and Lau 1998) and other empirical analyses (Shukla 1987; Rao and Goswami 1988): high SST in the Arabian Sea precedes strong monsoon rain which, in turn, precedes low SST in the autumn. Interestingly, the highest positive correlations of SST with the AIRI do not occur in the boreal spring immediately preceding the onset of the monsoons (Fig. 2d), but earlier in the preceding December–February (DJF; Fig. 2c). During the DJF season, 22% of the SST grid boxes within the Indian Ocean correlate with the AIRI above the 99% significance level, and 79% correlate higher than the 95% significance level.

When correlations of monthly mean SST are computed with the AIRI, the strongest correlation of an individual month SST with the AIRI occurs in the Arabian Sea (0.52) in December at the 4° × 4° grid cell centered at 20°N, 66°E. For 19 out of the 24 yr in which the December Arabian Sea SST was above the mean, the Indian summer rainfall was also above normal, and 16 out of the 26 yr in which the SST was below average also had below-average rainfall. In this manner, the December Arabian Sea SST, as defined above, appears to be a useful early predictor of monsoon strength. When the Arabian Sea SST at this location is averaged over DJF [the Arabian Sea (AS1) index; Table 1], its correlation with the AIRI reaches 0.53, and 18 out of the 24 yr with above-average AS1 index have above-average mean summer rainfall. On the other hand, 15 out of the 26 yr with below-average AS1 index have below-average rainfall. The AS1 index is plotted in Fig. 3a with the AIRI. Averaging SST over a larger region within the Indian Ocean yields slightly lower correlations.

Figure 2c also shows that there is also a high cor-

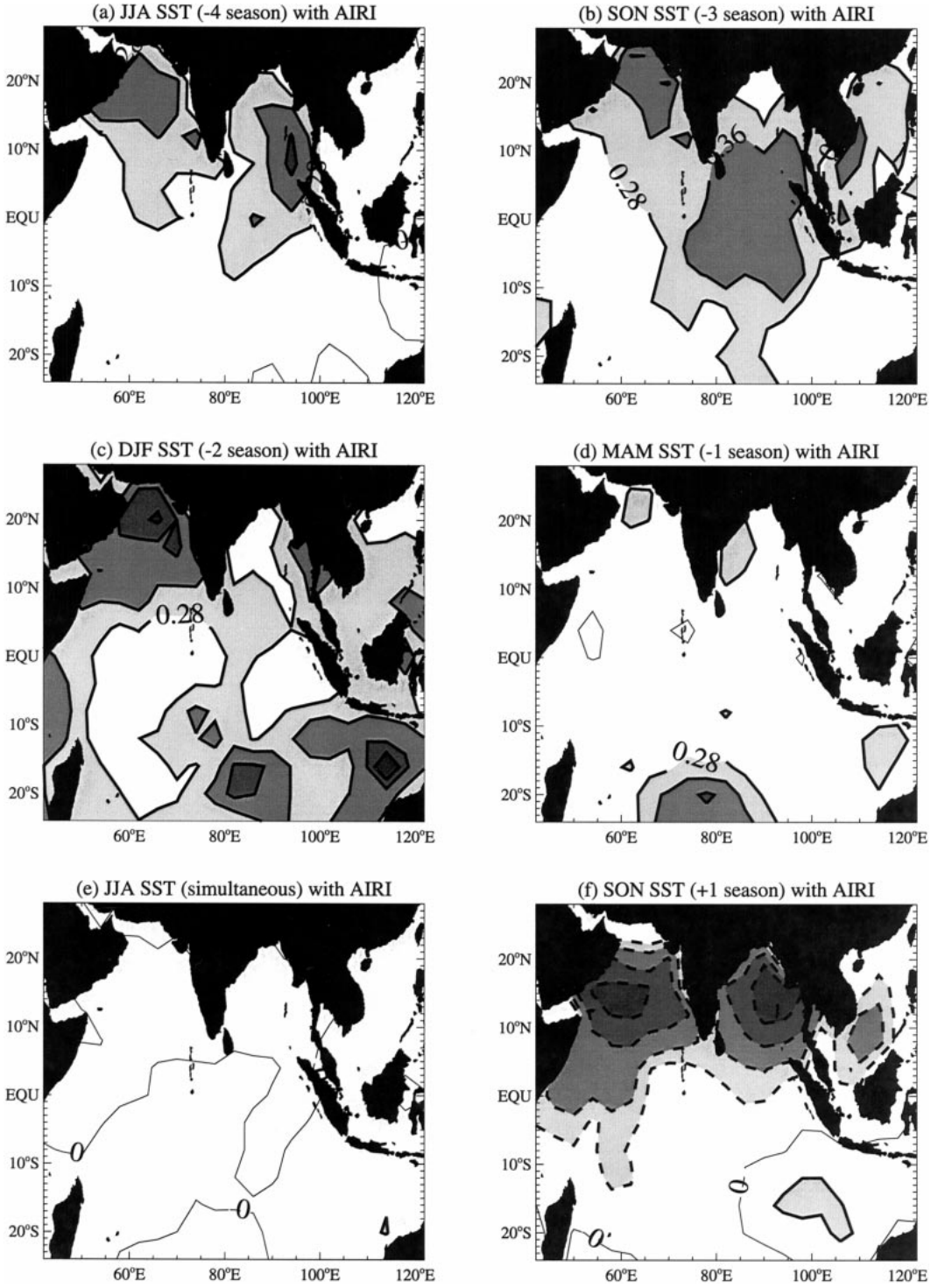

FIG. 2. Seasonal relationship of Indian Ocean SST with summer AIRI for the of period 1945–95. Correlations are shown between the JJAS AIRI and SST for seasons before and after the summer rainfall [(a)–(f)]. Contours are plotted for values −0.7, −0.6, 0.5, −0.36, −0.28, 0.0, 0.28, 0.36, 0.45, and 0.5. Significant contours are shaded (negative within dashed lines) for significance above 95% (0.28) and 99% (0.36).

TABLE 1. SST indexes.

Region	Lat, long	Months in index	SST index
AS (Arabian Sea)	20°N, 66°E	DJF	AS1
NWA (Northwest of Australia)	16°S, 114°E	DJF	NWA1
CIO (Central Indian Ocean)	4°N, 86°E	SON	CIO1

relation of DJF SST northwest of Australia (centered at 16°S, 114°E) with the AIRI. The DJF SST at this location [the northwest Australian (NWA1) index; Table 1] correlates to the AIRI at 0.58. This time series is plotted in Fig. 3b with the AIRI. Sixteen out of 21 years of above-average NWA SST have above-average India rainfall, and 16 out of 29 yr with below-average NWA SST have below-average rainfall.

We find the highest correlation of rainfall with the AIRI during the period of 1945–95 when we average the SST values for DJF from both the Arabian Sea and northwest Australia (AS1 + NWA1). The DJF SST timeseries from the Arabian Sea and northwest Australia each correlate with the AIRI at greater than 0.5, but correlate with each other at only 0.4, suggesting that SSTs at these locations reflect phenomena that are somewhat independent; thus, they yield the best correlation with the AIRI when they are combined. This combined time series and the AIRI are shown in Fig. 3c. The AS1 + NWA1 timeseries correlates with the AIRI at 0.66. In this case, 19 out of the 25 yr with above-average AS1 + NWA1 have above-average rainfall, and 15 out of the 25 years with below-average AS1 + NWA1 have below-average rainfall.

b. SST–Indian rainfall relationships, 1977–95

Because the Indian Ocean has undergone a significant warming after 1976 (Nitta and Yamada 1989; Terray 1994; Wang 1995), it is important to explore the affect of this climate shift on the SST–AIRI relationship. One study identifies a region in the central Indian Ocean (0°–5°N, 80°–85°E) where SST from 1967 to 1987 correlates with the AIRI at 0.75 (Sadhuram 1997). Although significant positive correlations between SST and the AIRI are seen in our analysis in the fall of the 1945–95 period (Fig. 2b), the magnitude of the correlation in this region is only 0.38. The discrepancy between the correlations seen by Sadhuram (1997) and our analysis can be explained by analyzing the SST–AIRI connection after 1976. We correlate SST with the AIRI as in the previous section (Fig. 2), but only for the years 1977–95 (Fig. 4). A region of much higher correlation ($r > 0.75$) is seen in the central Indian Ocean in September–November (SON) (Fig. 4b), agreeing with Sadhuram (1997). After 1977, the positive AS1 and NWA1 correlations are nearly the same as for the period of 1945–95 (Fig. 4c), but correlations are higher than the 99% significance level ($r = 0.60$) throughout most of the central Indian Ocean (Fig. 4b; Table 2). During the fall preceding the monsoon for 1977–95, 43% of the SST values correlate with the AIRI above the 95% significance level ($r = 0.48$) and 23% of the SST values correlate above the 99% level. The highest correlation ($r = 0.87$) of SON SST with the AIRI occurred at the location 4°N, 86°E (CIO1 index) (Table 1). This time series correlates strongly with the AIRI only after 1976 (Fig. 3d). Averaging over the region used by Sadhuram (1997) gave slightly lower correlations than the CIO1 index. When the CIO1, AS1, and NWA1 indexes are combined, the resulting timeseries has a correlation of 0.67 with the AIRI for the period of 1945–95 (Fig. 3e; Table 2) and correlates with the AIRI at 0.86 after 1976.

c. Tropospheric biennial oscillation

Figures 2 and 4 show that the correlations of SST with rainfall are generally positive preceding the onset of the monsoon and then subsequently become strongly negative. This is consistent with a negative feedback system (Meehl 1997) that could generate a biennial oscillation in monsoon strength. We subtract the November SST following the monsoon from the January SST preceding the monsoon and correlate this remainder with the AIRI (Fig. 5a). The feedback mechanism appears to have its strongest signature in the Arabian Sea, where January SST minus the following November SST correlates to the AIRI at 0.79.

Figure 5b shows the annual cycle of correlation between the AIRI and monthly SST from the aforementioned locations in the AS, NWA, and CIO. All three time series show positive correlations above the 99% significance level in boreal fall and winter preceding the monsoon. These positive correlations weaken in the spring preceding the monsoon and diverge somewhat during the summer monsoon. The correlations of the AS and the CIO monthly SST time series with rainfall rapidly become strongly negative in the fall following the monsoon, while the correlation with the NWA time series remains weakly positive. Correlation of the NWA SST with the AIRI gradually becomes negative in the boreal fall following the monsoon. Similarly, Nicholls (1983, his Fig. 1) found that correlations of Indonesian and Pacific SST in boreal fall and winter with the AIRI weaken and change sign in the winter and the early spring preceding the monsoon.

d. Relation to ENSO

Analyses of the dominant modes of global SST show a global influence of ENSO (e.g., Lanzante 1996; Tourre and White 1995). These studies find that SST anomalies in the Indian Ocean tend to lag those in the Pacific by about 3 months. We investigate the influence of ENSO on the Indian Ocean SST by correlating the SST time series at each point in the Indian Ocean with the monthly Niño-3 index (Fig. 6). The Indian Ocean SST has its highest simultaneous correlation (0.45) well above the

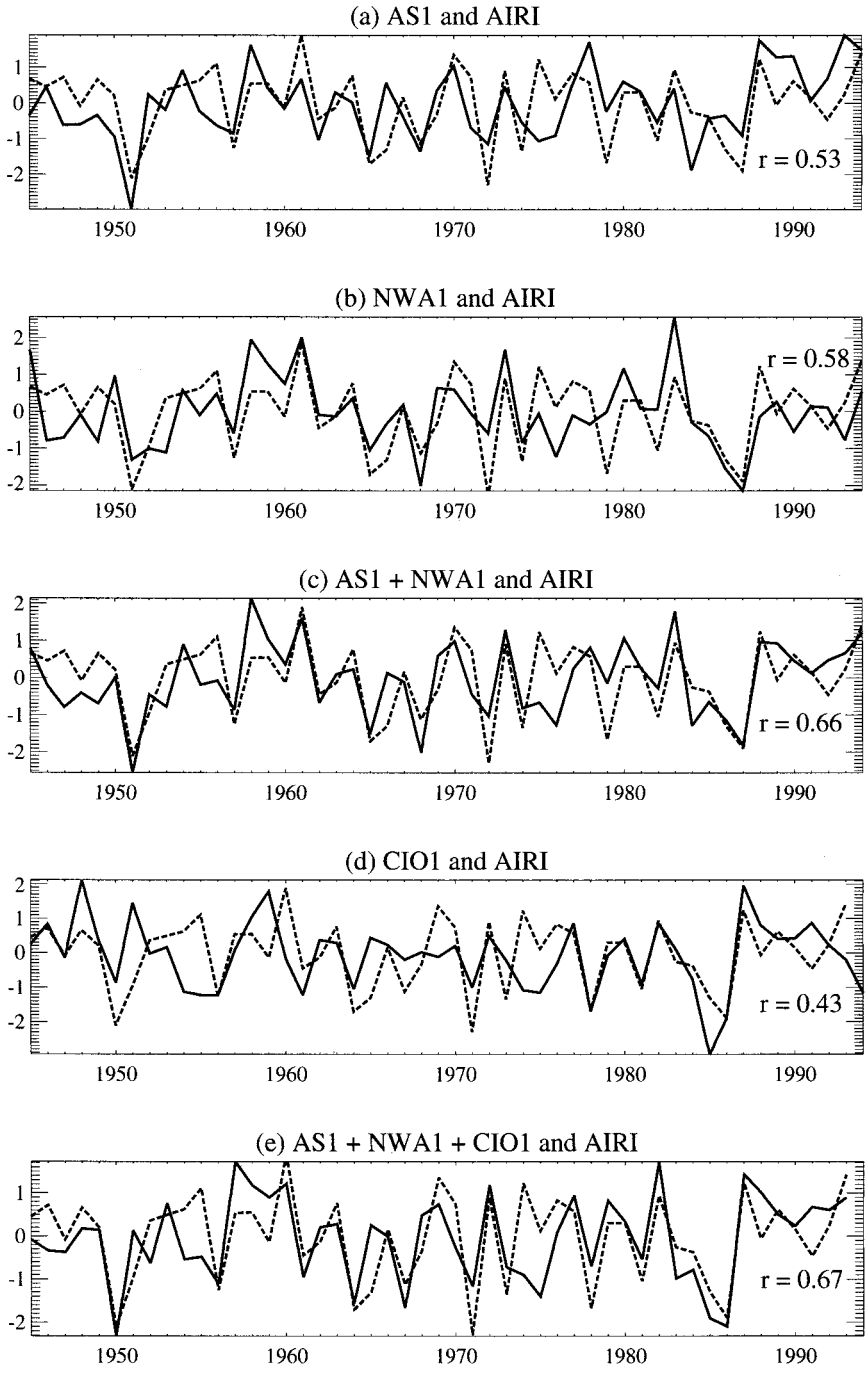

FIG. 3. Relationship of Indian Ocean SST indexes and the AIRI. The AIRI (dotted line) is plotted against (a) the AS1 index, (b) the NWA1 index, (c) the combined AS1 + NWA1 index, (d) the CIO1 index, and (e) the combined AS1 + NWA1 + CIO1 index. All indexes are normalized, and their correlations are shown in the panel.

99% significance level in a zonal band located to the south of Sri Lanka (Fig. 6a). This correlation is maximized and the significant region is broadened when the SST is lagged by four months (Fig. 6b; $r = 0.51$). When Niño-3 is correlated with SST after 1977, the region influenced by ENSO contracts substantially in both simultaneous and lagged correlation fields, although the magnitude of the highest correlations remain about the same (Figs. 6c,d). In general, therefore, ENSO has a weaker signal in the Indian Ocean after 1976.

The three SST indexes and combinations of each index were correlated to the simultaneous Niño-3 signal

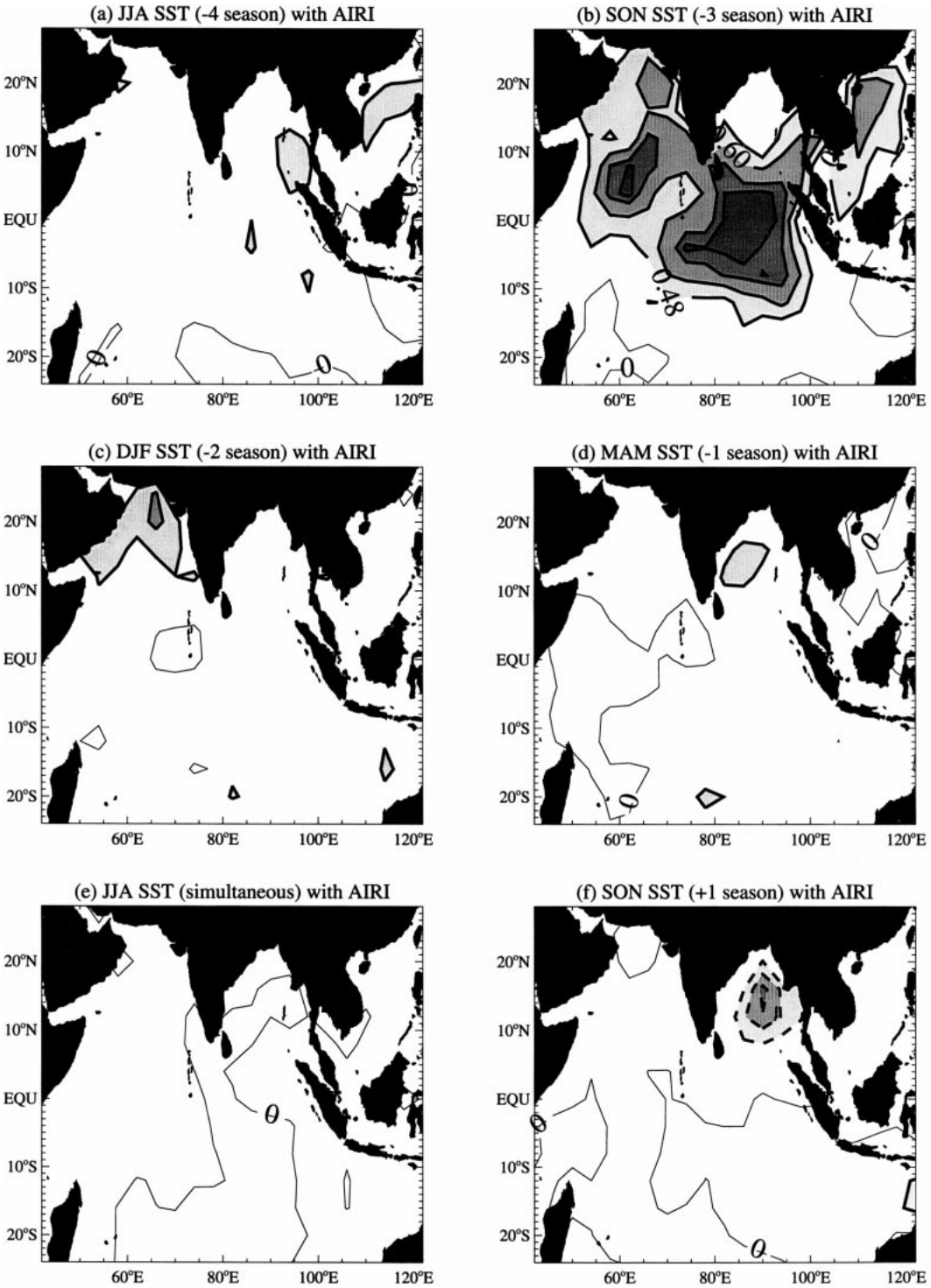

FIG. 4. Seasonal relationship of Indian Ocean SST with summer AIRI for the period of 1977–95. Correlations are shown between the JJAS AIRI and SST for seasons before and after the summer rainfall [(a)–(f)]. Contours are plotted for values −0.75, −0.7, 0.6, −0.48, 0.0, 0.48, 0.6, 0.7, and 0.75. Significant contours are shaded (negative within dashed lines) for significance above 95% (0.48) and 99% (0.6).

TABLE 2. Correlations of SST indices with Niño-3 and AIRI. Boldface indicates correlations that are significant at the 99% level, and italicized correlations are significant at the 95% level.

SST index	(a) Niño-3 1945–95	(b) Niño-3 1977–95	(c) AIRI 1945–95	(d) AIRI 1977–95	(e) AIRI 1945–95 Niño-3 removed	(f) AIRI 1977–95 Niño-3 removed
AS1	**0.39**	0.06	**0.53**	**0.63**	**0.52**	**0.63**
NWA1	**0.42**	*0.50*	**0.58**	*0.53*	**0.58**	*0.53*
CIO1	**0.38**	0.32	**0.43**	**0.87**	*0.32*	**0.66**
AS1 + NWA1	**0.48**	0.36	**0.66**	**0.75**	**0.67**	**0.76**
AS1 + CIO1	**0.46**	0.20	**0.57**	**0.82**	**0.54**	**0.76**
NWA1 + CIO1	**0.49**	0.46	**0.62**	**0.77**	**0.62**	**0.78**
AS1 + NWA1 + CIO1	**0.52**	0.36	**0.67**	**0.86**	**0.68**	**0.84**

for the years 1945–95 (Table 2, column a) and 1977–95 (Table 2, column b). For combinations of indexes for SON and DJF, such as AS1 + CIO1, Niño-3 was averaged over September through February. In agreement with previous studies, ENSO has a strong influence on Indian Ocean SST characteristics (Tourre and White 1995; Lanzante 1996). This influence is clearly seasonally modulated, as the correlation of Niño-3 with seasonal indexes tends to be higher than those with all monthly anomalies (shown in Fig. 6).

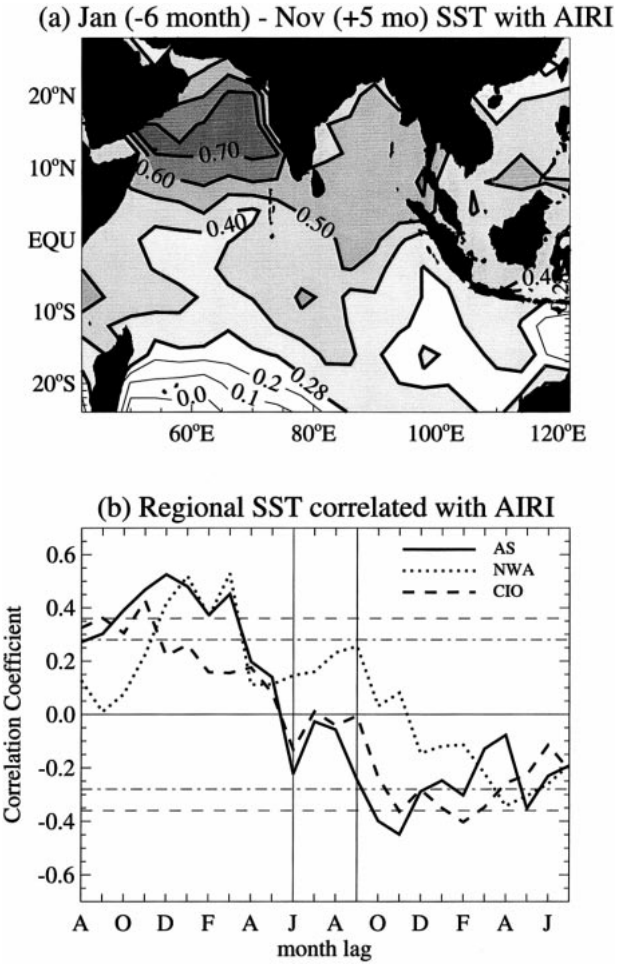

FIG. 5. (a) Correlation of Jan (year 0) minus the following Nov (year +1) SST with the AIRI for the period of 1945–95. Shaded regions denote significance above the 95% and 99% significance level. (b) Correlations of the AIRI with SST from the AS, NWA and the CIO are plotted for a 2-yr composite. The horizontal dashed lines represent the 95% and the 99% significance levels, and the vertical lines represent the beginning and end of the monsoon season.

To address if and how the Indian Ocean can affect the Asian monsoon independently from ENSO, we performed a regression analysis at each point in the Indian Ocean to remove the ENSO signal from the SST. The regression equation is derived from the definition of the correlation coefficient:

$$\text{SST(regressed)} = \text{SST} - \left[\frac{\sigma(\text{SST})}{\sigma(\text{Niño-3})}\right]\text{Niño-3}, \quad (1)$$

where σ(SST) is the standard deviation of the SST at each point and σ(Niño-3) is the standard deviation of the Niño-3 index. The resulting SST values are uncorrelated with Niño-3. We then correlated each month of the ''ENSO free'' SST data from 1945 to 1995 with the AIRI, as in section 3a. The results of the analysis are shown in Fig. 7. High positive correlations in winter and early spring are not reduced by the removal of the Niño-3 signal when compared with Fig. 2c (Fig. 7c; Table 2). This result is not surprising considering that the strongest effect of ENSO occurs in the CIO rather than the AS or NWA. With the removal of the Niño-3 signal, the correlation of the CIO index with the AIRI is reduced from 0.38 to 0.32. Thus, ENSO is contributing slightly to the correlation of central Indian Ocean SST with Indian rainfall. The negative correlations of SST with the AIRI in the fall following the monsoon are also reduced by the removal of the Niño-3 signal (Fig. 7f).

When the same correlation analysis in Fig. 7 is calculated for the years 1977–95, the results are quite different (Table 2, column f). The results of the analysis for the reduced data period is shown in Fig. 8. The removal of ENSO from the SST data greatly reduces the magnitude of the correlation of SON SST in the CIO (Fig. 8b) when compared with Fig. 4b. The correlation of the CIO1 was reduced from 0.87 to 0.66, implying that the CIO1 predictive relationship is influenced more strongly by ENSO after 1976. Although ENSO appears

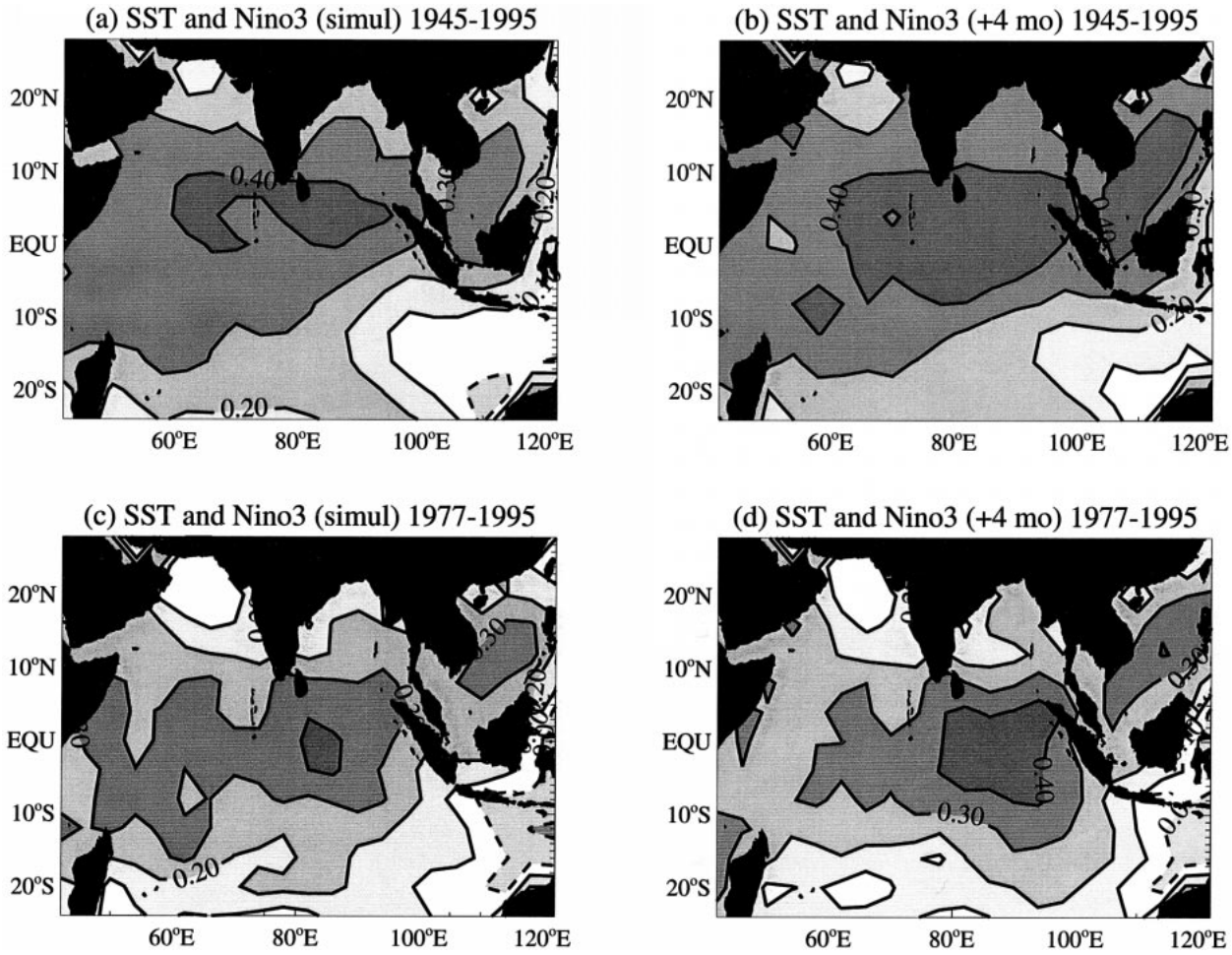

FIG. 6. Contours of correlations of Indian Ocean SST with (a) the simultaneous Niño-3 SST index for years 1945–95, (b) the Niño-3 SST index leading by 4 months, years 1945–95, (c) the simultaneous Niño-3 SST index for years 1977–95, and (d) the Niño-3 SST index leading by 4 months, years 1977–95.

to influence a smaller region of the Indian Ocean after 1976 (Fig. 6), the CIO remains well-correlated throughout the warming transition, and the CIO1 exhibits a much stronger correlation with the AIRI after 1976. ENSO has a stronger influence on the CIO1–AIRI relationship after 1976 despite the reduced spatial extent of its influence on the Indian Ocean.

4. Discussion

The research presented here raises a number of questions:

(i) *What is the temporal stability of the prediction of Indian monsoon rainfall using the SST indexes and how important is the 1976 shift compared to other periods?* Figure 9 shows sliding 18-yr correlations of SST with the AIRI for the AS1, NWA1, and CIO1 indexes. The AS1 and NWA1 correlate with the AIRI above the 95% level throughout most of the period from 1955 to 1984. On the other hand, the correlation of the CIO1 only becomes significant after 1976. With respect to the change in the CIO1–AIRI correlation, the 1976 shift appears to be a significant event.

To determine how the strength of the SST–AIRI correlation varies with ENSO, we examine the residuals of the AIRI–SST correlations. We normalize all SST indexes and their combinations and the AIRI timeseries by dividing them by their respective standard deviations. We then subtract the normalized AIRI from each SST index, providing residuals that represent the strength of the skill of the SST–AIRI correlations. A positive value of the residuals represents underestimation of Indian rainfall based on Indian Ocean SST predictions (i.e., more rain fell than was predicted), and a negative value represents overestimation. We compare these residuals to the normalized simultaneous Niño-3 index. The residuals of AS1, NWA1, and CIO1 correlate to Niño-3 at 0.23, 0.27, and 0.22, respectively (Fig. 10a–c). Although the positive correlations from individual regions are not significant, the residuals of AS1 + NWA1 and

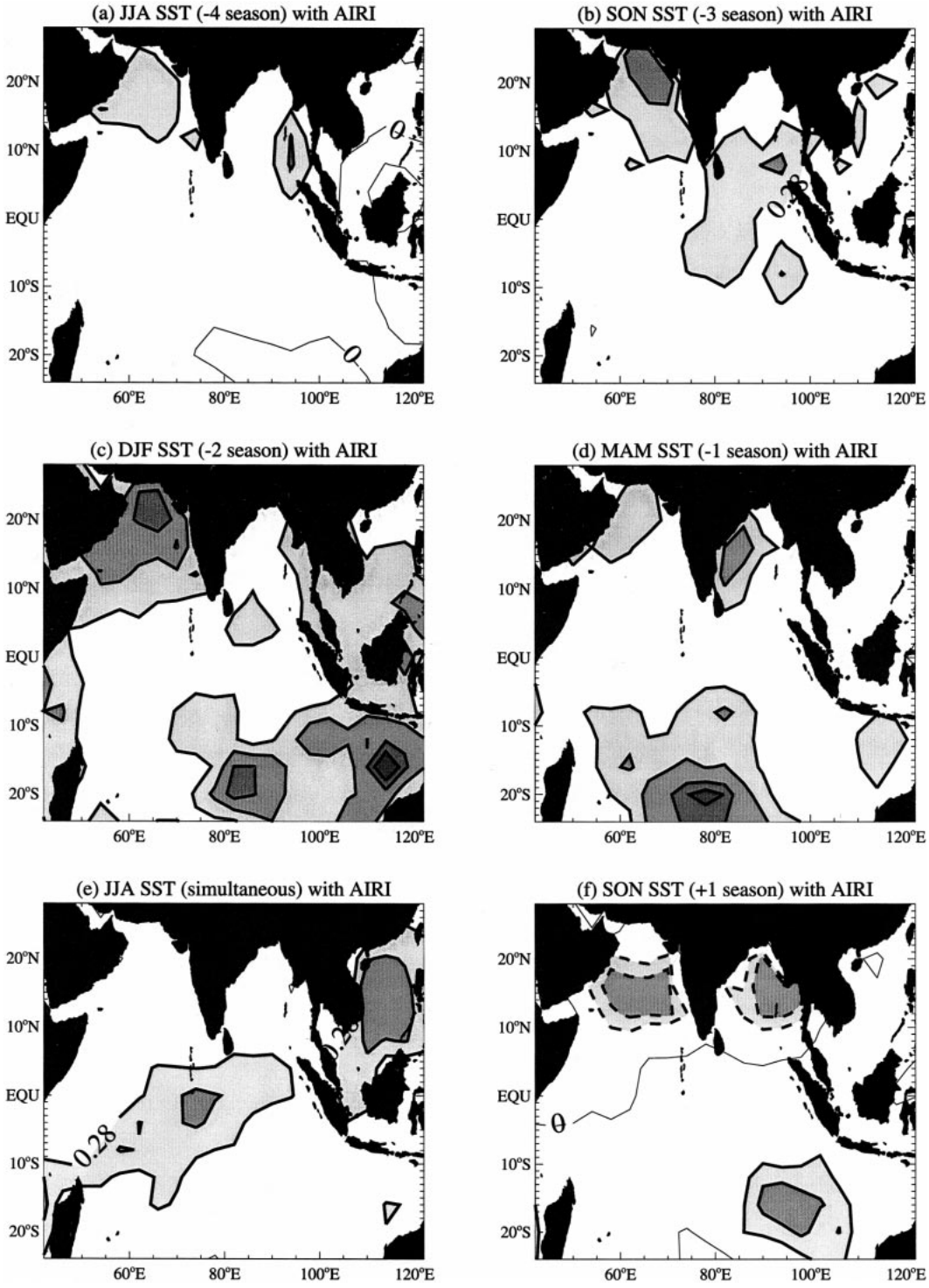

FIG. 7. Seasonal relationship of Indian Ocean SST with summer AIRI for the period of 1945–95 In contrast with Fig. 2, the simultaneous Niño-3 SST signal has been removed from the SST data. Correlations are shown between the JJAS AIRI and SST for seasons before and after the summer rainfall [(a)–(f)]. Contours are plotted for values −0.7, −0.6, 0.5, −0.36, −0.28, 0.0, 0.28, 0.36, 0.45, and 0.5. Significant contours are shaded (negative within dashed lines) for significance above 95% (0.28) and 99% (0.36).

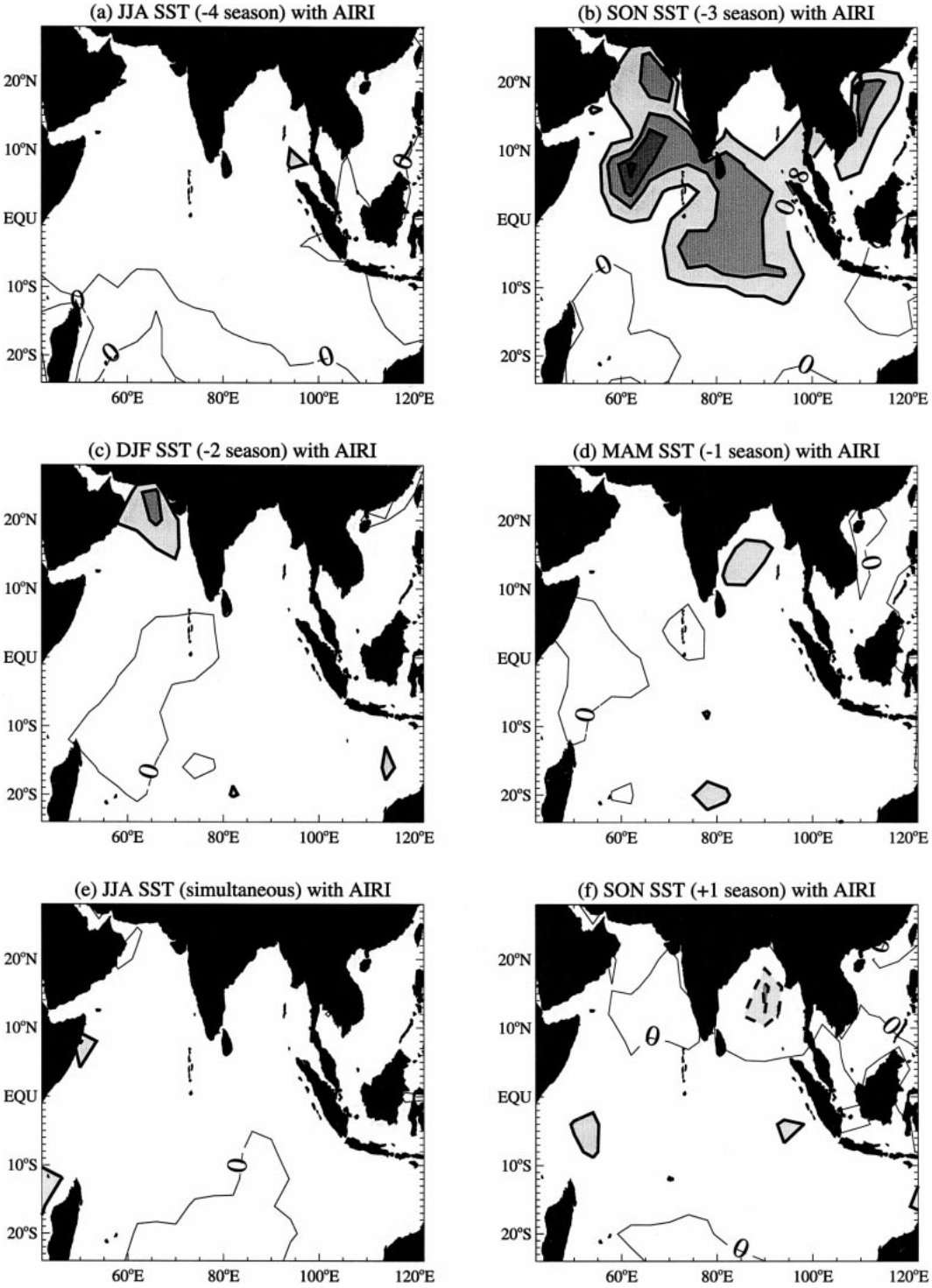

FIG. 8. Seasonal relationship of Indian Ocean SST with summer AIRI for the period of 1977–95. In contrast with Fig. 4, the simultaneous Niño-3 SST signal has been removed from the SST data. Correlations are shown between the JJAS AIRI and SST for seasons before and after the summer rainfall [(a)–(f)]. Contours are plotted for values −0.75, −0.7, 0.6, −0.48, 0.0, 0.48, 0.6, 0.7, and 0.75. Significant contours are shaded (negative within dashed lines) for significance above 95% (0.48) and 99% (0.6).

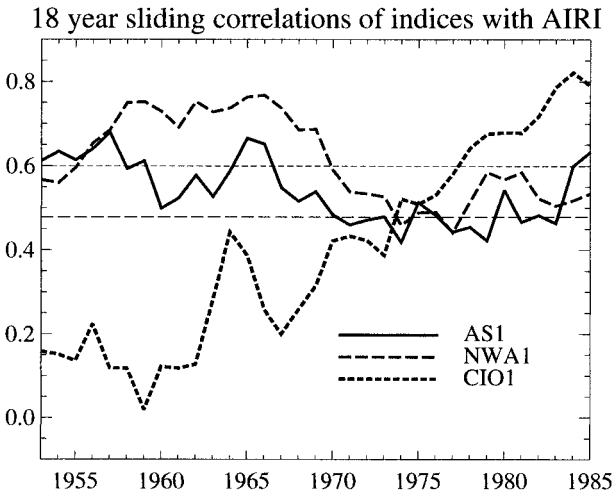

FIG. 9. Sliding correlations of the SST indexes with the AIRI with an 18-yr window. The horizontal dotted lines represent the 95% and 99% significance level.

AS1 + NWA1 + CIO1 correlate with Niño-3 at 0.38 and 0.39, respectively, which is significant at the 99% level (Figs. 10d,e). These results suggest that when Niño-3 is positive (El Niño years), the rainfall is often less than one would expect from SST prediction. Conversely, when Niño-3 is negative (La Niña), the rainfall is greater than that predicted by the combined indices. This result is not surprising, as El Niño is generally accompanied by a weak monsoon and La Niña is accompanied by a strong monsoon (Webster and Yang 1992; Webster et al. 1998). The residual of the CIO1 index is seen to correlate more strongly with Niño-3 after 1973. There is evidence that the structure and evolution of ENSO have undergone changes to the background state since 1976 (Wang 1995; Trenberth 1990), and our analysis shows that Indian Ocean warming strengthened dramatically at that time (Fig. 1). If the 1976 shift in Indian Ocean climate affected the interaction of ENSO and the Indian monsoon and if this change represents a stable configuration, then the high correlation of the AIRI with the CIO1 index should yield accurate predictions of rainfall if the post-1976 climate regime persists. However, future climate shifts may further influence the interaction among Indian Ocean SST, ENSO, and the monsoon, which could disrupt the predictive relationships we document here. Thus, changes to the background climate state influence predictive relationships between Indian Ocean SST and the AIRI.

Table 2 shows that although the AS1 + NWA1 index has the highest correlation of Indian rainfall from 1945 to 1995, after 1976, the CIO1 index gives the best prediction of rainfall. The residuals in Fig. 10 represent the accuracy of the linear prediction of monsoon rainfall from the SST indexes. To a first order, the AS1 + NWA1 residuals do not show dramatic changes through time, suggesting that a prediction scheme based on these data is relatively stable. To the extent that the residuals correlate with ENSO over part of this record, ENSO is a source of noise in the prediction that varies through time.

The higher correlation of the CIO1 residual with the Niño-3 index after 1976 occurs following the period of greatest warming of the central Indian Ocean (Figs. 1a,d). We suggest this change results from the shift in the base state of the Indian Ocean. Similarly, Salinger et al. (1995) see a change in the relationship between Australian rainfall and ENSO following 1976, which they attribute to changes in the state of the Indian Ocean.

(ii) *Are the correlations between SST and rainfall due to the biennial nature of the monsoon?* For the ocean to produce a biennial oscillation of monsoon strength, as discussed by Meehl (1997), not only must a negative feedback on SST follow the monsoon, but the resulting SST anomalies must persist until the next monsoon season. In Fig. 5b, the correlation of the Arabian Sea SST with the AIRI is negative at the 99% significance level in the October and November following the monsoon but becomes less negative leading into the next monsoon season. Although this lack of persistence does not rule out the possibility of the Arabian Sea producing biennial monsoon variability, it suggests that the resulting biennial signal from the Arabian Sea may not be strong. The autocorrelation of the AIRI lagged by one year is only −0.137. The 2-yr lagged autocorrelation of the AIRI is near zero (−0.06) These results suggest that in both the AIRI and the Arabian Sea, biennial activity is not strong enough to generate the SST–AIRI relationships we observe. The AS1 index correlates with the previous year with a coefficient of 0.16. The NWA1 index exhibits a 1-yr lagged autocorrelation of 0.05, and the CIO1 has a 1-yr lagged autocorrelation of 0.15. Thus, bienniality is not measurably contributing to the predictability of the AIRI by SST indexes from these regions.

(iii) *What mechanism produces the high correlation of the regional SST indexes with summer Indian rainfall?* At this stage we have not proposed a mechanism explaining why fall and winter SST in the Indian Ocean at these specific locations are good predictors of Indian rainfall, but any possible mechanism must satisfy certain conditions. The positive correlations of SST at the three locations with the AIRI display the strongest signal in the fall and winter preceding the monsoon and later weaken in the spring. If SST was directly influencing the monsoon through evaporation and moisture supply, one would expect positive correlations to persist and even strengthen throughout the spring, leading to the onset of rainfall. Therefore, these SST anomalies must influence the monsoon through a delayed coupled ocean–atmospheric feedback. Webster et al. (1999) show evidence of a low-frequency coupled ocean–atmosphere mode that bridges forcing from one year to the next, independently of ENSO. This mode may be important for our results as the predictive capability of the AS1 and NWA1 indexes arises independently of any

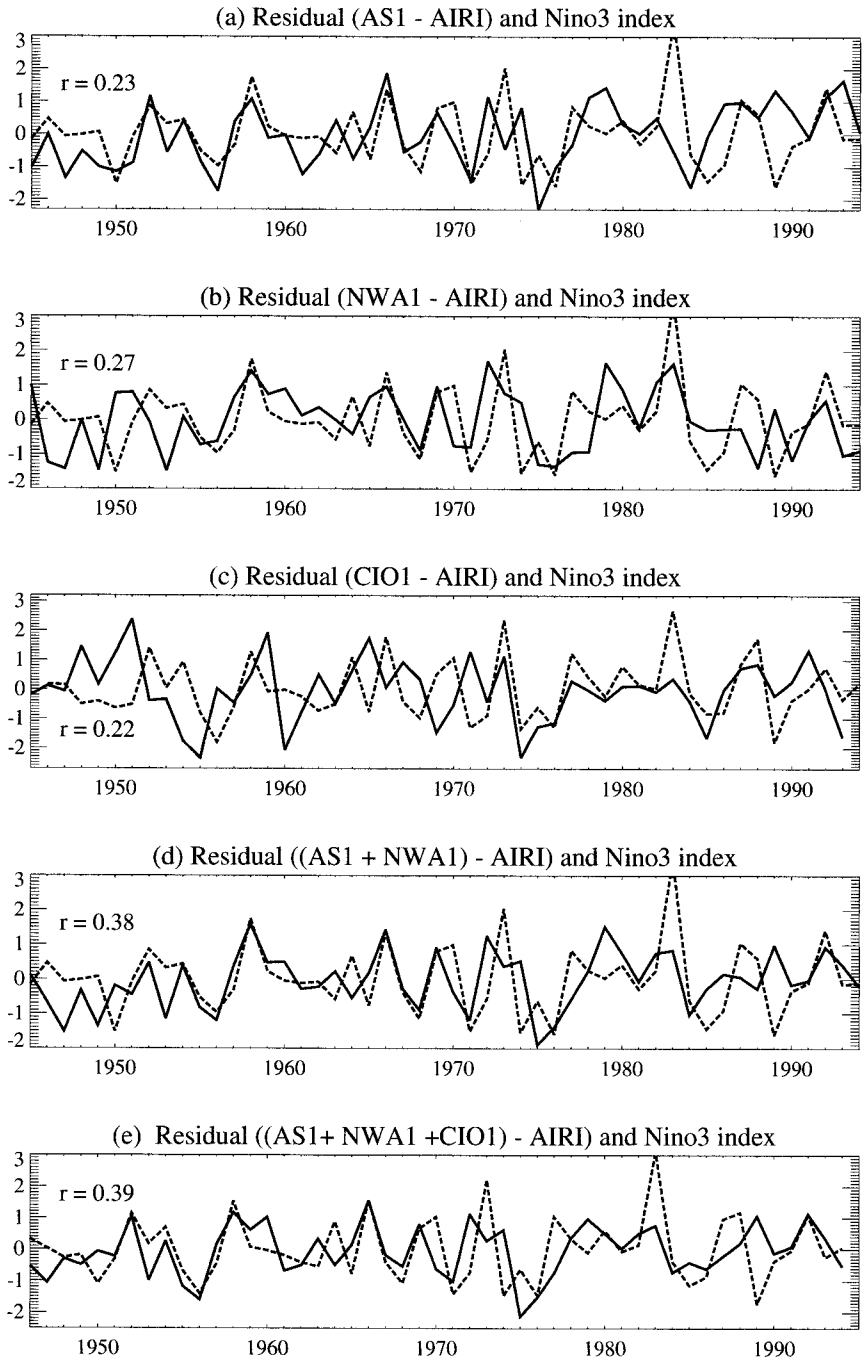

FIG. 10. (a) Residual of the normalized AS1 index minus the normalized AIRI index (solid line). The residual correlates with the Niño-3 SST index (dashed line) at 0.23. (b) Residual of the normalized NWA1 index minus the normalized AIRI index (solid line). The residual correlates with the Niño-3 SST index (dashed line) at 0.27. (c) Residual of the normalized CIO1 minus the normalized AIRI index (solid line). The residual correlates with the Niño-3 SST index (dashed line) at 0.22. (d) Residual of the normalized AS1 + NWA1 index minus the normalized AIRI index (solid line). The residual correlates with the Niño-3 SST index (dashed line) at 0.38. (e) Residual of the normalized AS1 + NWA1 + CIO1 minus the normalized AIRI index (solid line). The residual correlates with the Niño-3 SST index (dashed line) at 0.39. Residuals show the degree of skill of the AIRI–SST index correlations. A positive residual represents an overestimation of the AIRI by the index and vice versa.

ENSO influence. In addition, winter and early spring SST anomalies set the strength of the monsoon gyre, and monsoon rain in equatorial regions exists some months before rainfall occurs in India. Overall, it is clear that the identification of processes that produce these long-lead indexes is essential. Identifying mechanisms that satisfy these criteria is a focus of further investigation.

5. Conclusions

This study explores the annual cycle of SST–Indian monsoon rainfall relationships. We build upon the foundation laid by Shukla and Mooley (1987), Rao and Goswami (1988), Harzallah and Sadourny (1997), and Sadhuram (1997) that Indian Ocean SST is significantly correlated with the all-India rainfall index several months preceding the onset of the monsoon. We extend these studies by examining the interdecadal variability of this relationship and its connection to ENSO, noting especially the change of the character of the correlations after 1976. We draw the following conclusions.

1) Indexes composed of winter SST, the AS1, NWA1, and combined AS1 + NWA1 correlate significantly with subsequent AIRI ($r = 0.53$, 0.58, 0.66, respectively), and this relationship is stable over the 50-yr period of our analysis.
2) A fall SST index from the central Indian Ocean (CIO1) also correlates significantly with the AIRI, but the high correlation appears to develop only after 1976 ($r = 0.87$), with insignificant correlations in earlier years.
3) Combining SST indexes from all three regions gives an index that correlates with the AIRI at $r = 0.67$ and is stable throughout the period of analysis (Fig. 3e). Because this index can be constructed for a given year by the March preceding the summer monsoon, it holds great potential for contributing to a long-lead forecasting scheme for all-India rainfall.
4) The residual from the correlation between the AIRI and the combined SST indexes correlates with the simultaneous Niño-3 at 0.39, which implies that ENSO indicators can improve upon a predictive scheme that uses only Indian Ocean SSTs.
5) The 1976 climate shift, seen in the datasets of both Indian and Pacific Oceans, influences these relationships as follows:
   (a) The central Indian Ocean becomes strongly coupled to the AIRI following a period of weak correlation.
   (b) After 1976, the residual of the CIO1 linear prediction of the AIRI correlates more strongly to ENSO than previously.
   (c) These results are consistent with the idea that Pacific variability, particularly the 1976 shift, influences the relationship between Indian Ocean SST and the Indian monsoon.
6) Monsoon prediction strategies need to take into account the decadal changing background climate state, as background changes may enhance or degrade predictive relationships. Whether the 1976 shift represents a shift to a new state in which relationships are stable or a time of continually changing climate in which the relationships we have identified are variable remains to be determined.
7) Physical mechanisms of these relationships need to be established in order to evaluate the stability of monsoon–SST relationships.

Our findings, when used in conjunction with other aforementioned empirical predictive schemes, may contribute to improved early predictions of the Indian monsoon. Future predictive schemes will use datasets of many variables coupled with a better understanding of the ocean–atmosphere–land feedback mechanisms that give rise to strong early correlations. It is necessary to explore the SST–AIRI relationship before 1945 to understand further the interdecadal variability of the ocean–atmosphere interaction and the warming trend. Our future work will focus on the identification of physical mechanisms using additional datasets such as sea level pressure, wind, precipitation, and sea level height. Ultimately, we need to understand the physical mechanisms that drive the observed correlations in order to identify a predictive scheme that is stable and therefore useful in a time of changing background climate.

Acknowledgments. This research was supported by the National Science Foundation Grants OCE-9614137 (to J. E. Cole) and ATM-9525847 (to P. J. Webster). Special thanks to Dr. C. Torrence for assistance in acquiring the datasets used in this study and Drs. S. Dixit and A. Moore for discussion. The manuscript was improved by the comments of anonymous reviewers.

REFERENCES

Allan, R. J., J. A. Lindesay, and C. J. Reason, 1995: Multidecadal variability in the climate system over the Indian Ocean region during the Austral summer. *J. Climate*, **8,** 1853–1873.

Barnett, T. P., L. Dumenil, U. Schlese, E. Roekler, and M. Latif, 1989: The effect of Eurasian snow cover on regional and global climate variations. *J. Atmos. Sci.*, **46,** 661–685.

Bjerknes, J., 1969: Atmospheric teleconnections from the equatorial Pacific. *Mon. Wea. Rev.*, **97,** 163–172.

Bottomley, M., C. K. Folland, J. Hsiung, R. E. Newell, and D. E. Parker, 1990: *Global Ocean Surface Temperature Atlas 'GOSTA'*. Joint Meteor. Massachusetts Institute of Technology Atlas, HMSO, 20 pp.

Graham, N. E., 1994: Decadal-scale climate variability in the tropical and North Pacific during the 1970s and 1980s: Observations and model results. *Climate Dyn.*, **10,** 135–162.

Harzallah, R., and R. Sadourny, 1997: Observed lead-lag relationships between Indian summer monsoon and some meteorological variables. *Climate Dyn.*, **13,** 635–648.

Hastenrath, S., 1986: On climate prediction in the tropics. *Bull. Amer. Meteor. Soc.*, **67,** 696–702.

——, 1987: On the prediction of India summer rainfall anomalies. *J. Climate Appl. Meteor.*, **26,** 847–857.

——, 1994: *Climate Dynamics of the Tropics.* Kluwer Academic Publishers, 488 pp.
Joseph, P. V., and P. V. Pillai, 1984: Air–sea interaction on a seasonal scale over north Indian Ocean—Part 1: Inter-annual variations of sea surface temperature and Indian summer monsoon rainfall. *Mausam,* **35,** 323–330.
Kershaw, R., 1988: Effect of a sea surface temperature anomaly on a prediction of the onset of the southwest monsoon over India. *Quart. J. Roy. Meteor. Soc.,* **114,** 325–345.
Lanzante, J. R., 1996: Lag relationships involving tropical sea surface temperatures. *J. Climate,* **9,** 2568–2578.
Lindzen, R. S., and S. Nigam, 1987: On the role of sea surface temperature gradients in forcing low-level winds and convergence in the Tropics. *J. Atmos. Sci.,* **44,** 2418–2436.
Meehl, G. A., 1987: The annual cycle and interannual variability in the tropical Pacific and Indian Ocean region. *Mon. Wea. Rev.,* **115,** 27–50.
——, 1997: The south Asian monsoon and the tropospheric biennial oscillation. *J. Climate,* **10,** 1921–1943.
Mooley, D. A., and B. Parthasarathy, 1984: Fluctuations in All-India summer monsoon rainfall during 1871–1978. *Climatic Change,* **6,** 287–301.
Nicholls, N., 1983: Predicting Indian monsoon rainfall from sea-surface temperature in the Indonesia-north Australia area. *Nature,* **306,** 576–577.
Nitta, T., and S. Yamada, 1989: Recent warming of tropical sea surface temperature and its relationship to the Northern Hemisphere circulation. *J. Meteor. Soc. Japan,* **67,** 375–383.
Parker, D. E., M. Jackson, and E. B. Horton, 1995: The GISST2.2 sea surface temperature and sea-ice climatology. Tech. Rep. CRTN 63, Hadley Centre for Climate Prediction and Research, Meteorological Office, 35 pp. [Available from Hadley Centre for Climate Prediction and Research, Meteorological Office, London Rd., Bracknell, Berkshire RG122SY, United Kingdom.]
Parthasarathy, B., H. F. Diaz, and J. K. Eischeid, 1988: Prediction of all-India summer monsoon rainfall with regional and large-scale parameters. *J. Geophys. Res.,* **93,** 5341–5350.
——, K. Rupa Kumar, and D. R. Kothawale, 1992: Indian summer monsoon rainfall indices: 1871–1990. *Meteor. Mag.,* **121,** 174–186.
Rao, K. G., and B. N. Goswami, 1988: Interannual variations of sea surface temperature over the Arabian Sea and the Indian monsoon: A new perspective. *Mon. Wea. Rev.,* **116,** 558–568.
Sadhuram, Y., 1997: Predicting monsoon rainfall and pressure indices from sea surface temperature. *Curr. Sci.,* **72,** 166–168.
Salinger, M. J., and Coauthors, 1995: Biennial oscillation associated with the East Asian summer monsoon and tropical sea surface temperatures. *J. Meteor. Soc. Japan,* **73,** 105–124.
Shukla, J., 1975: Effect of Arabian sea-surface temperature anomaly on Indian summer monsoon: A numerical experiment with the GFDL model. *J. Atmos. Sci.,* **32,** 503–511.
——, 1987: Interannual variability of monsoons. *Monsoons,* J. S. Fein and P. L. Stephens, Eds., John Wiley and Sons, 399–464.
——, and D. A. Mooley, 1987: Empirical prediction of the summer monsoon rainfall over India. *Mon. Wea. Rev.,* **115,** 695–703.
——, and M. J. Fennessy, 1994: Simulation and predictability of monsoons. *Proc. Int. Conf. on Monsoon Variability and Prediction,* Tech. Rep. WCRP-84, Geneva, Switzerland, World Climate Research Programme, 567–575.
Sperber, K. R., and T. N. Palmer, 1996: Interannual tropical rainfall variability in general circulation model simulations associated with the Atmospheric Model Intercomparison Project. *J. Climate,* **9,** 2727–2750.
Terray, P., 1994: An evaluation of climatological data in the Indian Ocean area. *J. Meteor. Soc. Japan,* **72,** 359–385.
Torrence, C., and P. J. Webster, 1999: Interdecadal changes in the ENSO–monsoon system. *J. Climate,* **12,** 2679–2690.
Tourre, Y., and W. White, 1995: ENSO signals in global upper-ocean temperature. *J. Phys. Oceanogr.,* **25,** 1317–1332.
Trenberth, K. E., 1990: Recent observed interdecadal climate changes in the Northern Hemisphere. *Bull. Amer. Meteor. Soc.,* **71,** 988–993.
——, and T. J. Hoar, 1996: The 1990–1995 El Niño–Southern Oscillation event: Longest on record. *Geophys. Res. Lett.,* **23,** 57–60.
Troup, A. J., 1965: The Southern Oscillation. *Quart. J. Roy. Meteor. Soc.,* **91,** 490–506.
Vernekar, A. D., J. Zhou, and J. Shukla, 1995: The effect of Eurasian snow cover on the Indian monsoon. *J. Climate,* **8,** 248–266.
Wang, B., 1995: Interdecadal changes in El Niño onset in the last four decades. *J. Climate,* **8,** 267–285.
Webster, P. J., 1987: The elementary monsoon. *Monsoons,* J. S. Fein and P. L. Stephens, Eds., John Wiley and Sons, 399–464.
——, and S. Yang, 1992: Monsoon and ENSO: Selectively interactive systems. *Quart. J. Roy. Meteor. Soc.,* **118,** 877–926.
——, V. O. Magana, T. N. Palmer, J. Shukla, R. A. Tomas, M. Yanai, and T. Yasunari, 1998: Monsoons: Processes, predictability, and the prospects for prediction. *J. Geophys. Res.,* **103,** 14 451–14 510.
——, A. M. Moore, J. P. Loschnigg, and R. R. Leben, 1999: Coupled ocean–atmosphere dynamics in the Indian Ocean during 1997–98. *Nature,* **40,** 356–360.
World Climate Research Programme (WCRP), 1992: Simulation of interannual and intraseasonal monsoon variability. Tech. Document WMO/TD 470, 145 pp.
Wu, M.-C., 1985: On the prediction of the Indian summer monsoon. *Pap. Meteor. Res.,* **8,** 35–43.
Yanai, M., and C. Li, 1994: Mechanism of heating and the boundary layer over the Tibetan Plateau. *Mon. Wea. Rev,* **122,** 305–323.
Yang, S., 1996: ENSO-snow-monsoon associations and seasonal-to-interannual predictions. *Int. J. Climatol,* **16,** 125–134.
——, and K. M. Lau, 1998: Influences of sea surface temperature and ground wetness on the Asian summer monsoon. *J. Climate,* **11,** 3230–3246.
Yasunari, T., A. Kitoh, and T. Tokioka, 1991: Local and remote responses to excessive snow mass over Eurasia appearing in the northern spring and summer climate—A study with the MRIH-GCM. *J. Meteor. Soc. Japan,* **69,** 473–487.